Available online at www.sciencedirect.com
ScienceDirect
Optik 121 (2010) 426–434
Optik Optics
www.elsevier.de/ijleo

Determining the time–frequency parameters of low-power bright picosecond optical pulses by using the interferometric technique

Alexandre S. Shcherbakov[a,*], Ana Luz Muñoz Zurita[a], Alexey Yu. Kosarsky[b,1], Joaquin Campos Acosta[c,2]

[a]*Department of Optics, National Institute for Astrophysics, Optics, and Electronics (INAOE), A.P. 51 and 216, Puebla, Pue. 72000, Mexico*
[b]*LLC "Petro", Peterhoff Chausse 71, Saint-Petersburg 198206, Russian Federation*
[c]*Department of Metrology, Institute for Applied Physics (IFA-CSIC), Serrano 144, Madrid 28006, Spain*

Received 7 March 2008; accepted 6 July 2008

Abstract

We present an approach to the characterization of low-power bright picosecond optical pulses with an internal frequency modulation simultaneously in both time and frequency domains in practically much used case of the Gaussian shape. This approach exploits the Wigner time–frequency distribution, which can be found for these bright pulses by using a novel interferometric technique under our proposal. Then, the simplest two-beam scanning Michelson interferometer is selected for shaping the field-strength auto-correlation function of low-power picosecond pulse trains. We are proposing and considering in principle the key features of a new experimental technique for accurate and reliable measurements of the train-average width as well as the value and sign of the frequency chirp of pulses in high-repetition-rate trains. This technique is founded on an ingenious algorithm for the advanced metrology, assumes using a specially designed supplementary semiconductor cell, and suggests carrying out a pair of additional measures with exploiting this semiconductor cell. Such a procedure makes possible constructing the Wigner distribution and describing the above-listed time–frequency parameters of low-power bright picosecond optical pulses. In the appendix, we follow one of possible avenues for deriving the joint Wigner time–frequency distribution via choosing the Weil's correspondence between classical functions and operators.

Keywords: Bright picosecond optical pulse; Wigner time–frequency distribution; Interferometric technique

1. Introduction

The problem of characterizing solitary bright picosecond pulses meets, broadly speaking, the fundamental difficulty determined eventually by the necessity of converting the needed data from faster all-optical format (peculiar to a frequency range of about 1 THz) to much slower electronic format due to operating all the modern opto-electronic equipment over just electronic signals whose frequencies

*Corresponding author. Tel./fax: +52 222 2472940.
E-mail addresses: alex@inaoep.mx (A.S. Shcherbakov), azurita@inaoep.mx (A.L. Muñoz Zurita), alexey.kosarsky@jt-int.com (A.Y. Kosarsky), joaquin.campos@ita.cetef.csic.es (J. Campos Acosta).
[1]Tel.: +7 812 5343334.
[2]Tel.: +34 915618806; fax: +34 914117651.

0030-4026/$ - see front matter
doi:10.1016/j.ijleo.2008.07.033

usually do not exceed of about 10 GHz. This difficulty cannot be resolved directly, because our equipment cannot now and will not be able in the nearest future operate in a terahertz frequency range. In other words, one can say that the problem of characterizing is related to the problem of adequate photon-to-electron conversion in real, i.e. determined by light, time scale. That is why, in fact, all the attempts of developing the measurement techniques in this area were directed on resolving this fundamental difficulty [1–4]. The most progressive approach, which is able to simplify potential solution of the above-mentioned difficulty, is based up to now on so-called train-average characterization of picosecond pulse sequences rather than solitary pulses. However, the train-average approach, on the one hand, needs the regular trains of identical picosecond pulses and, on the other hand, requires exploiting some mechanism of sampling. While generating the regular trains of more or less identical picosecond pulses is not a considerable problem for the modern optics, choosing the sampling mechanism does not look like too obvious and/or quite trivial step first of all because such mechanisms can be rather different from each other. The most developed techniques, providing similar sampling all-optically, are based on shaping various correlations between different parts of different picosecond pulses in the same train [5–8]. Together with this, the most popular among these correlations are auto-correlations of the second order, which are simple enough to be generated by the simplest two-beam scanning Michelson interferometer. Nevertheless, besides their simplicity, auto-correlations of the second order allow us to identify even the train-average pulse shape not always due to ambiguity in identification of the internal frequency modulation (or the frequency chirp) of pulses in a train. For instance, in the particular case of low-power picosecond pulses, the difficulties grow dramatically, because the majority of potentially available non-linear-optic approaches became to be practically unsuitable. In principle, all-optical conversions make it possible to perform many transformations of pulses to keep the mainly important details inherent in the optical pulses of picosecond range, so that one could mention first of all interferometric techniques [7–10].

The presented work develops the above-described avenue in practically much used case of low-power picosecond pulses with the Gaussian shape. For this purpose, at first the problem is formulated in terms of the joint Wigner time–frequency distributions for Gaussian pulses [11]. Initially, we consider such distributions for the slowly varying amplitudes and then, generalize them on the Gaussian pulses with a high-frequency filling. In both these cases, the products of the half-width for the spectral contour at a level of $1/e$ and the pulse half-width at the same level with the contribution from frequency modulation of a pulse are of main interest. The developed analysis makes it possible to interpret potential experimental data in terms of the Wigner distributions and/or restore these distributions using the experimental results. Together with this, the corresponding approach to the field-strength auto-correlation function of the second order is formulated in the same terms as well. Finally, we propose a novel interferometric technique of measuring the train-average pulse width as well as the value and sign of the frequency chirp inherent in low-power picosecond optical pulses belonging to high-repetition-rate trains. Basic peculiarities of the technique under proposal are connected with rather specific algorithm of measurements having a two-beam interferometry into its background, with exploiting a specially designed supplementary semiconductor cell, and with carrying out two additional measures involving this semiconductor cell into the scheme of a two-beam scanning Michelson interferometer. In the appendix, one of possible modern versions of deriving the joint Wigner time–frequency distribution is considered.

2. The Wigner distribution for a Gaussian pulse

The complex amplitude of a solitary optical pulse with Gaussian shape of envelope can be written as

$$A_{\mathrm{G}}(t) = \exp\left[-\frac{(1+\mathrm{i}b)t^2}{2T^2}\right], \tag{1}$$

where T is the Gaussian pulse half-width measured at a level of $1/e$ for the intensity contour and b is the parameter of the frequency modulation. In this case, the joint Wigner time–frequency distribution, see Eq. (A.13), is given by

$$W_{\mathrm{G}}(t,\omega) = \frac{T}{\sqrt{\pi}}\exp\left[-\frac{t^2}{T^2} - \left(\omega T + \frac{bt}{T}\right)^2\right]. \tag{2}$$

The Wigner distribution for the Gaussian pulse is positive-valued. When $T = 1$ and $b = 0$, Eq. (2) gives the distribution, which is symmetrical relative to repositioning the variables t and ω. With decreasing the parameter b, the energy distribution concentrates in a bandwidth corresponding the chirp-free spectrum whose center lies along the line $\omega = bt/T^2$. A few examples of the time–frequency distribution $W_{\mathrm{G}}(t,\omega) = \pi^{-1/2}\exp\left[-t^2 - (\omega + bt)^2\right]$, defined by Eq. (2) with $T = 1$ are presented in Fig. 1.

Integrations in Eqs. (A.15) give the partial one-dimensional Wigner distributions for the Gaussian pulse over the time or frequency separately

$$|A_{\mathrm{G}}(t)|^2 = \int_{-\infty}^{\infty} W_{\mathrm{G}}(t,\omega)\,\mathrm{d}\omega = \exp\left(-\frac{t^2}{T^2}\right), \tag{3}$$

$$|S_{\mathrm{G}}(\omega)|^2 = \int_{-\infty}^{\infty} W_{\mathrm{G}}(t,\omega)\,\mathrm{d}t = \frac{T^2}{\sqrt{1+b^2}}\exp\left(-\frac{T^2\omega^2}{1+b^2}\right). \tag{4}$$

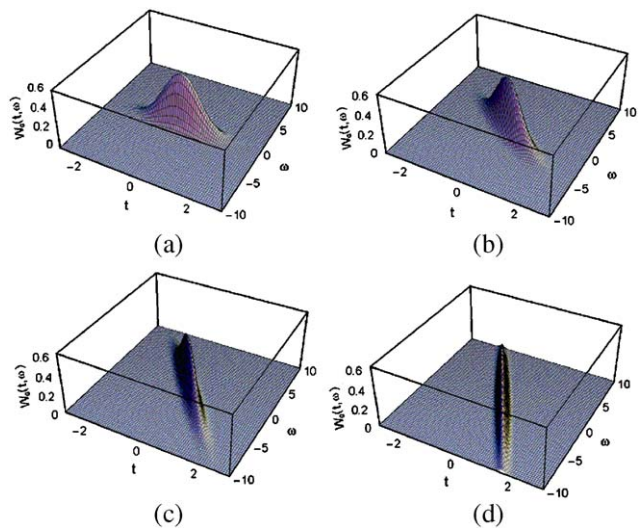

Fig. 1. The Wigner time–frequency distribution for the Gaussian pulse with $T = 1$ and the varying parameter b: (a) $b = 0$, (b) $b = 2$, (c) $b = 4$, and (d) $b = 6$.

It is seen from Eq. (4) that to reach a level of $1/e$ one need vary the variable ω from $-T^{-1}\sqrt{1+b^2}$ to $T^{-1}\sqrt{1+b^2}$, so that the variation $\Delta\omega = T^{-1}\sqrt{1+b^2}$ means actually the half-width of the spectral contour at a level of e^{-1}. Thus, one can determine the product

$$\Delta\omega T = \sqrt{1+b^2}. \tag{5}$$

In the particular case of $b = 0$ (i.e. in the absence of the frequency chirp or the phase modulation), one yields $\Delta\omega T = 1$ for the Gaussian pulse. Nevertheless, in general case, $b \gg 1$, so the product $\Delta\omega T$ can far exceed unity. A few examples of the time and frequency distributions, determined by Eqs. (3) and (4) with $T = 1$ are shown in Fig. 2.

3. The Gaussian pulse with a high-frequency filling

Now, one can take the case of Gaussian pulse with the slowly varying amplitude and with a high-frequency filling by the optical carrier frequency $\Omega \gg 1$

$$U(t) = \exp\left(-\frac{t^2}{2T^2}\right)\cos\left(\Omega t + \frac{bt^2}{2T^2}\right). \tag{6}$$

The corresponding intensity distribution, instead of a smooth contour described by Eq. (3) for $I(t) = |A_G(t)|^2$, includes now some oscillations and is given by

$$J(t) = |U(t)|^2 = \exp\left(-\frac{t^2}{T^2}\right)\cos^2\left(\Omega t + \frac{bt^2}{2T^2}\right). \tag{7}$$

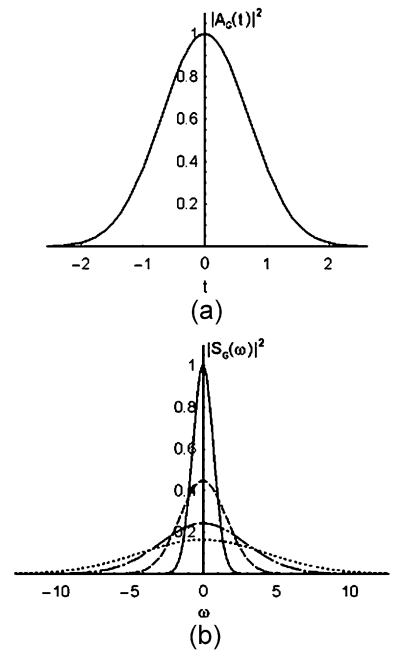

Fig. 2. The Gaussian pulse with $T = 1$: the power density profile (a) and the spectral density profiles (b) with the varying parameter of the frequency chirp: solid line for $b = 0$, dashed line for $b = 2$, dash-dotted line for $b = 4$, and dotted line for $b = 6$.

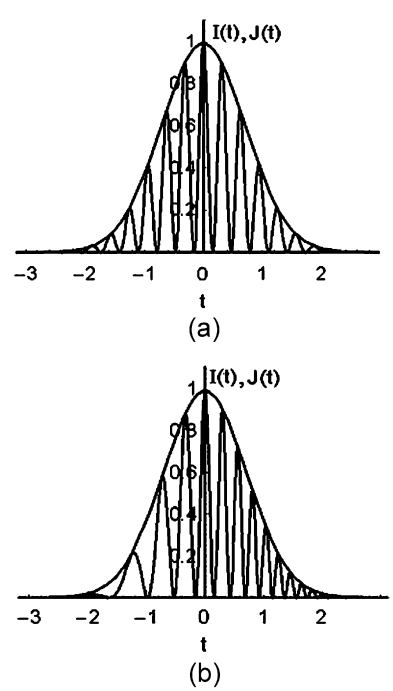

Fig. 3. The plots of $I(t)$ and $J(t)$ with: (a) $b = 0$, $T = 1$, $\Omega = 10$; (b) $b = 4$, $T = 1$, $\Omega = 10$.

The smooth contours $I(t)$ and the oscillating distributions $J(t)$ are shown in Fig. 3. One can see from Fig. 3. that the half-width has the same value T for these two plots. Then, one can consider the complex spectrum contour.

Performing the Fourier transform of Eq. (6), one can find

$$B(\omega) = T\sqrt{\frac{\pi}{2}}\left\{\frac{1}{\sqrt{1-\mathrm{i}b}}\exp\left[-\frac{T^2(\omega+\Omega)^2}{2(1-\mathrm{i}b)}\right] + \frac{1}{\sqrt{1+\mathrm{i}b}}\exp\left[-\frac{T^2(\omega-\Omega)^2}{2(1+\mathrm{i}b)}\right]\right\}. \quad (8)$$

The spectral intensity contour is now given by the following expression:

$$\begin{aligned} J(\omega) &= |B(\omega)|^2 \\ &= T^2\frac{\pi}{2}\left\{\frac{1}{\sqrt{1-\mathrm{i}b}}\exp\left[-\frac{T^2(\omega+\Omega)^2}{2(1-\mathrm{i}b)}\right] + \frac{1}{\sqrt{1-\mathrm{i}b}}\exp\left[-\frac{T^2(\omega-\Omega)^2}{2(1-\mathrm{i}b)}\right]\right\} \\ &\quad\times\left\{\frac{1}{\sqrt{1+\mathrm{i}b}}\exp\left[-\frac{T^2(\omega+\Omega)^2}{2(1+\mathrm{i}b)}\right]\right\}. \end{aligned} \quad (9)$$

This expression has obviously real form

$$\begin{aligned} J(\omega) = |B(\omega)|^2 = \frac{\pi T^2}{2}\Bigg\{&\frac{1}{\sqrt{1+b^2}}\exp\left[-\frac{T^2(\omega-\Omega)^2}{1+b^2}\right] \\ &+\frac{1}{\sqrt{1+b^2}}\exp\left[-\frac{T^2(\omega+\Omega)^2}{1+b^2}\right] \\ &+\left(\frac{2}{1+b^2}\exp\left[-\frac{T^2(\omega^2+\Omega^2)}{1+b^2}\right]\right. \\ &\times\left.\left\{\cos\left[\frac{bT^2(\omega^2+\Omega^2)}{1+b^2}\right] - b\sin\left[\frac{bT^2(\omega^2+\Omega^2)}{1+b^2}\right]\right\}\right)\Bigg\}. \end{aligned} \quad (10)$$

Now, one can consider the case of $\omega \approx \Omega$ with $\Omega \gg 1$. In this case, $(\omega+\Omega)^2 \gg (\omega-\Omega)^2$ and $(\omega^2+\Omega^2) \gg (\omega-\Omega)^2$, so that Eq. (8) give

$$B(\omega) \approx T\sqrt{\frac{\pi}{2(1+\mathrm{i}b)}}\exp\left[-\frac{T^2(\omega-\Omega)^2}{2(1+\mathrm{i}b)}\right]$$

and

$$B^*(\omega) \approx T\sqrt{\frac{\pi}{2(1-\mathrm{i}b)}}\exp\left[-\frac{T^2(\omega-\Omega)^2}{2(1-\mathrm{i}b)}\right],$$

while Eq. (10) saves only the first term in the external brackets. Consequently, the spectral intensity contour can be approximately estimated by

$$J(\omega) = |B(\omega)|^2 \approx \frac{\pi T^2}{2\sqrt{1+b^2}}\exp\left[-\frac{T^2(\omega-\Omega)^2}{1+b^2}\right], \quad (11)$$

which is presented in Fig. 4. The width of this contour is determined by $\Delta\Omega = \omega - \Omega$, so one can write

$$\Delta\Omega T = \sqrt{1+b^2}. \quad (12)$$

Eq. (12) is quite similar to Eq. (5) and has the same meaning.

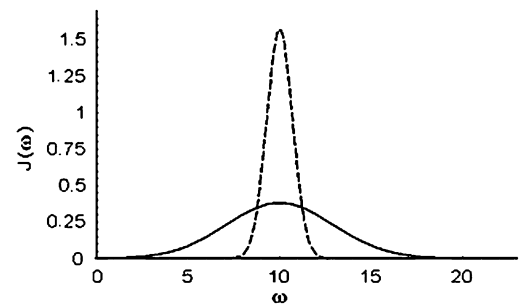

Fig. 4. Spectral intensity of Gaussian pulses: $b = 0$, $T = 1$, $\Omega = 10$ – dashed line; $b = 4$, $T = 1$, $\Omega = 10$ – solid line.

Finally, the field-strength auto-correlation function can be estimated. For this purpose, one can consider a two-beam scanning Michelson interferometer, which is the simplest optical auto-correlator. Such a device makes it possible to register the field-strength auto-correlation function, which can be exploited via the inverse Fourier transform for finding the spectral power density $|S(\omega)|^2$ and measuring the width of the spectral contour. In so doing, one has to use a square-law photodiode detecting an interference of two incident field strengths $U(t)$ and $U(t-\tau)$, where the delay time τ of the second field can be varied by the corresponding movable mirror of the scanning interferometer. The issuing electronic signal is proportional to the energy E under registration, if the integration time of that photodiode is sufficiently long. Generally, this energy is proportional to the value

$$E \sim \int_{-\infty}^{\infty}[U(t)+U(t-\tau)]^2\,\mathrm{d}t \sim G_0(0) + 2G_\mathrm{A}(\tau), \quad (13)$$

where $G_0(0)$ is a background and

$$\begin{aligned} G_\mathrm{A}(\tau) &= \int_{-\infty}^{\infty}[U(t)\times U(t-\tau)]\,\mathrm{d}t \\ &= \frac{1}{2\pi}\int_{-\infty}^{\infty}|B(\omega)|^2\exp(-\mathrm{i}\omega t)\,\mathrm{d}\omega, \end{aligned} \quad (14)$$

Eq. (14) is true only when the field strength $U(t)$ is real-valued; for example, for the Gaussian pulse described by Eq. (6). So, using Eq. (14), the function $G_\mathrm{A}(\tau)$ can be calculated due to the Fourier transform of the spectral intensity contour

$$\begin{aligned} G_\mathrm{A}(\tau) &= \frac{1}{2\pi}\int_{-\infty}^{\infty}|B(\omega)|^2\exp(-\mathrm{i}\omega t)\,\mathrm{d}\omega \\ &= \frac{T\sqrt{\pi}}{2}\exp\left(\frac{-\tau^2}{4T^2}\right)\left[\exp\left(\frac{-b^2\tau^2}{4T^2}\right)\cos(\Omega\theta)\right. \\ &\quad\left.+\frac{1}{\sqrt[4]{1+b^2}}\exp\left(\frac{-T^2\Omega^2}{1+b^2}\right)\cos\left(\frac{b\tau^2}{4T^2}-\frac{bT^2\Omega^2}{1+b^2}+\frac{b}{2}\right)\right]. \end{aligned} \quad (15)$$

The analysis shows that the second term in the square brackets of Eq. (15) is negligible in comparison with

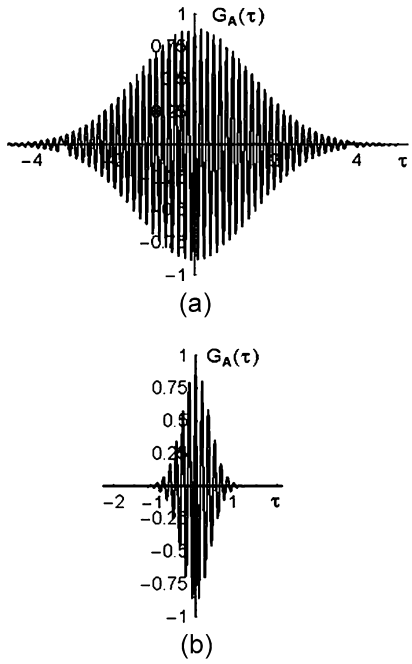

Fig. 5. Field-strength auto-correlation functions for the Gaussian pulses with: (a) $b = 0$, $T = 1$, $\Omega = 40$; (b) $b = 4$, $T = 1$, $\Omega = 40$.

the first one, so the approximate expression for the field-strength auto-correlation function can be written as

$$G_{\mathrm{A}}(\tau) \approx \frac{T\sqrt{\pi}}{2} \exp\left[-\frac{(1+b^2)\tau^2}{4T^2}\right] \cos(\Omega\theta). \tag{16}$$

Two traces for this reduced auto-correlation function are shown in Fig. 5. That is why the width of the field-strength auto-correlation function can be rather accurate estimated through estimating the exponential term in Eq. (16). A level of $1/e$ will be reached with

$$\tau = \tau_0 = 2T/\sqrt{1+b^2}. \tag{17}$$

Consequently, τ_0 is the half-width of the field-strength auto-correlation function at a level of $1/e$.

4. A new technique of measuring the train-average pulse width as well as the value and sign of the frequency chirp of picosecond optical pulses in high-repetition-rate trains

In many cases, for example, with the investigations of evolving the optical solitons in active and passive waveguide structures, a simple method is frequently required for measuring current time–frequency parameters of low-power pico and sub-picosecond optical pulses traveling in high-repetition-rate trains. Most widely used is a method based on the formation of a train-average auto-correlation function of the field strength, which is coupled through the Fourier transform with the spectral power density. From the recorded power spectral density, one can determine an average width of the radiation spectrum. However, in this case, information on the average field phase is lost and it is impossible to determine the time variation of the field amplitude $A(t)$. Exact determination of the train-average pulse duration from the width of the radiation spectrum is only possible when the shape of pulse envelope is known a priori and, in addition, the pulse spectrum is limited [8]. An approximate estimation of the pulse duration is also correct, if the frequency chirp is sufficiently small [9]. In the general case, it is necessary either to pass to determination of the intensity auto-correlation or cross-correlation [10] functions, or to make special measurements to obtain information on the field phase, which often require the application of rather complicated experimental facilities or special computer algorithms [12–14]. Here, we demonstrate an opportunity of providing experimental conditions, under which the train-average auto-correlation function of the field strength can serve as a source of exact and reliable information on the average values of both duration and frequency chirp of a low-power optical pulses traveling in high-repetition-rate trains.

We proceed from the assumption that all pulses in a train are identical pulses having a Gaussian envelope described by Eq. (1) with the amplitude $A_0 = \sqrt{P}$, where P is the incoming pulse peak power. These assumptions are not specific for the proposed method and are typical of most of the other measurement methods [8,12]. For a Gaussian envelope, the relationships between the train-average pulse parameters T and b and the width τ_0 of the corresponding auto-correlation function measured on a level of $1/e$ are given by Eq. (17).

Usually, the real-time auto-correlation function of the field strength averaged over a train of optical pulses is obtained with a scanning Michelson interferometer [9,10], which allows measuring the value of τ_0. However, it follows from formula (17) that information on the width τ_0 of the field-strength auto-correlation function is insufficient to determine the time–frequency parameters of the pulse train. That is why one can propose performing two additional measurements of the auto-correlation function width with the help of a scanning Michelson interferometer. During the second and third measurements, supplementary optical components, changing the parameters T and b in a predetermined way but not influencing the envelope of the investigated pulses, should be placed in front of the beam-splitting mirror of the interferometer. The auto-correlation function widths τ_m ($m = 1,2$) obtained from the repeated measurements are coupled with the new values of the pulse duration T_m and the frequency chirp b_m through formula (17). We assume that $T_m = \alpha_m T_0$ and $b_m = b_0 + \beta_m$, where T_0 and b_0 are unknown values of

the parameters T and b, while the quantities α_m and β_m are determined by supplementary optical components. Using the above-noted relations, one can write two different algebraic quadratic equations for a quantity of b_0. The corresponding solutions are given by the formulas

$$b_0 = (q_m\alpha_m^2 - 1)^{-1}\left[\beta_m \pm \sqrt{q_m\alpha_m^2(\beta_m^2+2) - (q_m^2\alpha_m^4+1)}\right], \tag{18}$$

where $q_m = \tau_0^2/\tau_m^2$ and τ_m is the width of the field strength auto-correlation function obtained without supplementary optical components. For $(m = 1,2)$, Eq. (18) gives four values of b_0, of which two coincide with each other and correspond to just the true value of the train-average frequency chirp of the pulses. The proposed measurement method allows one to determine not only the value, but the sign of the frequency chirp as well, which is often impossible even with the help of substantially more complicated methods, such as, for example, the method described in Ref. [13]. Once the pulse frequency chirp b_0 is determined, one can use formula (18) to calculate the pulse duration T by using τ_0 and $b = b_0$.

For the supplementary electronically controlled optical component, one can propose exploiting a specific device based on an InGaAsP single-mode traveling-wave semiconductor laser heterostructure, which is quite similar to a saturable-absorber laser [15] with clarified facets. This device comprises two domains, see Fig. 6. Domain I of the linear amplification controlled by pumping current J_m has the length L_1 and is characterized by the low-signal gain factor $\kappa_1(J_m)$. Domain II of a fast-absorption saturation, created by a deep implantation of oxygen ions into the output facet of the heterostructure, has the length L_2 and is characterized by the low-signal absorption factor κ_2 and the saturation power P_S. Domain I is able to modify the peak power P_m of pulses entering domain II, so that $P_m = P\exp[\kappa_1(J_m)L_1]$. The peak power P_m determines, in its turn, the values of the parameters α_m and β_m, reflecting the action of domain II on the pulses. In the low-signal case, one can use the relations [15].

$$\text{(a)}\quad \alpha_m = (\rho P_m\sqrt{2}+1)^{-1/2},$$
$$\text{(b)}\quad \beta_m = -\zeta\rho P_m\sqrt{2}, \tag{19}$$

where ζ is the line-width enhancement factor [16], which is usually in the range $\zeta = 3-8$, and

$$\rho = (2P_S)^{-1}[\kappa_1(J_m)L_1] \tag{20}$$

is the absorption parameter which may be of the order of $\rho \leqslant 1\,\mathrm{W}^{-1}$. Such a device makes possible performing the repeated measurements without re-adjusting the optical circuit and ensures additions $\beta_m \leqslant 5$ to the frequency chirp [15].

Fig. 7 demonstrates variation in the auto-correlation function after inserting the supplementary electronically controlled semiconductor optical cell into the measurement circuit. It shows a pair of simulated oscillograms for the auto-correlation functions of Gaussian pulses formed by a scanning Michelson interferometer without (a) and with (b) inserted semiconductor cell for the case of $\beta_m = -2$. Arrows mark a level of $\exp(-0.5) \approx 0.606$ used to determine the value of T. The numerical simulation has been performed for a signal-to-noise ratio of 10, which corresponds to rather typical experimental conditions [17–19]. The data obtained from triply repeated measurements of T allows us to determine the pulse duration in a range of 1–50 ps and the pulse frequency chirp in a range of 0–$\pm$10 with an account for the chirp sign. The measurement accuracy is

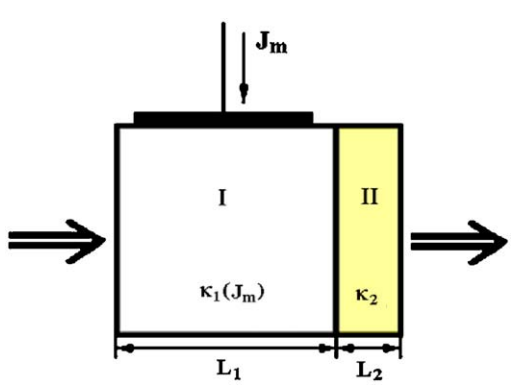

Fig. 6. Design of the supplementary semiconductor cell: **I** is the domain of linear amplification controlled by the pump current J; **II** is the domain with a fast-saturable absorption.

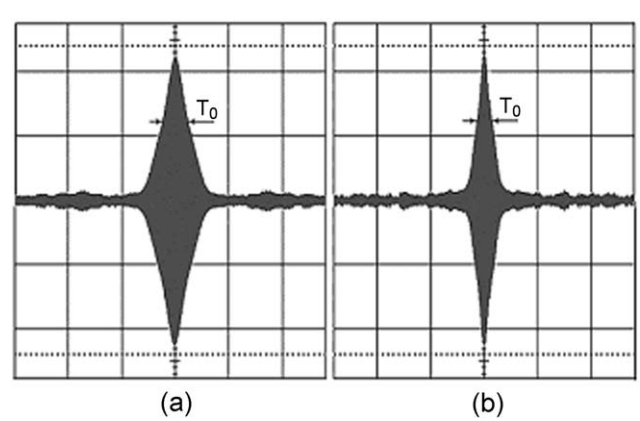

Fig. 7. Results of numerical simulation of forming the auto-correlation functions by the scanning Michelson interferometer: (a) without and (b) with an supplementary semiconductor cell introduced into the measurement circuit.

determined by the instability of radiation source and uncertainty of the scanning circuit characteristics as well as by the errors arising during the recording. The total measurement errors for both the pulse duration and the frequency chirp do not exceed 5%.

5. Conclusion

We consider the above-presented material as a stimulating contribution to the development of the advanced metrology. Such a viewpoint is based on the two well-determined propositions. The first of them is represented by our theoretic approach to the characterization of low-power bright picosecond optical pulses with an internal frequency modulation simultaneously in time and frequency domains. This proposition exploits the joint Wigner time–frequency distribution, which can describe the width and the frequency chirp of optical pulse in a unified format. The case, being practically much used, of Gaussian shape when the Wigner distribution is positive has been taken, and the peculiarities for just the Gaussian pulses with a high-frequency filling have been followed in details in both time and frequency domains as well as in terms of the field-strength auto-correlation function. The second proposition is related to the principles of creating the joint Wigner time–frequency distribution by the methods of modern experimental technique. We have proposed and considered conceptually the key features of a new interferometric method elaborated explicitly for accurate and reliable measurements of the train-average width as well as the value and sign of the frequency chirp in bright picosecond optical pulses in high-repetition-rate trains. For this purpose, a two-beam scanning Michelson interferometer has been chosen for obtaining the field-strength auto-correlation function of low-power picosecond pulse trains. The proposed technique is founded on an ingenious algorithm of metrology, assumes using a specially designed two-domain supplementary semiconductor cell, and suggests carrying out a pair of additional measures with exploiting this semiconductor cell, whose properties have been physically described as well. The procedure makes possible constructing the current Wigner distribution in real-time scale, which is rather desirable practically, and thus describing low-power bright picosecond optical pulses simultaneously in both time and frequency domains.

Acknowledgments

This work was financially supported by CONACyT, Mexico (Project no. 61237) and the National Institute for Astrophysics, Optics & Electronics, Mexico (Opto-Electronic Project).

Appendix A. Originating the joint Wigner time–frequency distribution

When the spectrum of signal varying in time is the subject of interest, it is rather worthwhile to refer to applying some joint function of the time and frequency, which would be able to describe the intensity distribution of this signal simultaneously in time domain as well as in frequency one. Such a distribution gives us opportunities for determining a relative part of energy at a given frequency in the required temporal interval or for finding the frequency distribution at a given instant of time.

The method of deriving the time–frequency distribution can be based on usage of the corresponding characteristic function. Let us assume that some time–frequency distribution $W(t,\omega)$ exists and presents a function of two variables t and ω.

The characteristic function $M(\theta,\tau)$ inherent in this distribution can be written as mathematical expectation of the value $\exp(\mathrm{i}\theta t+\mathrm{i}\tau\omega)$, i.e. as

$$M(\theta,\tau) = \langle \exp(\mathrm{i}\theta t + \mathrm{i}\tau\omega)\rangle = \int_{-\infty}^{\infty}\int_{-\infty}^{\infty} W(t,\omega)\exp(\mathrm{i}\theta t + \mathrm{i}\tau\omega)\,\mathrm{d}t\,\mathrm{d}\omega. \quad (A.1)$$

In its turn, the time–frequency distribution $W(t,\omega)$ can be found from the characteristic function $M(\theta,\tau)$ as

$$W(t,\omega) = \frac{1}{4\pi^2}\int_{-\infty}^{\infty}\int_{-\infty}^{\infty} M(\theta,\tau)\exp(-\mathrm{i}\theta t - \mathrm{i}\tau\omega)\mathrm{d}\theta\,\mathrm{d}\tau. \quad (A.2)$$

Due to the characteristic function is some averaged value, one can use quantum mechanics method of the associated operators with ordinary variables. If we have the function $g_1(t)$ depending only on the time t, the average value for this function can be calculated by two ways, namely, exploiting the complex amplitude $A(t)$ of a signal or its complex spectrum $S(\omega)$ as

$$\langle g_1(t)\rangle = \int_{-\infty}^{\infty} g_1(t)|A(t)|^2\,\mathrm{d}t = \int_{-\infty}^{\infty} S^*(\omega) g_1\left(\mathrm{i}\frac{d}{d\omega}\right) S(\omega)\,\mathrm{d}\omega \quad (A.3)$$

because the time can be represented by the operator $\mathrm{i}d/\mathrm{d}\omega$ in the frequency domain. Then, for the function $g_2(\omega)$ depending only on the frequency ω, the average value can be estimated by

$$\langle g_2(\omega)\rangle = \int_{-\infty}^{\infty} g_2(t)|S(\omega)|^2\,\mathrm{d}\omega = \int_{-\infty}^{\infty} A^*(t) g_2\left(-\mathrm{i}\frac{d}{\mathrm{d}t}\right) A(t)\,\mathrm{d}t \quad (A.4)$$

because the frequency is represented by the operator $-\mathrm{i}d/\mathrm{d}t$ in the time domain as well. Consequently, one can combine the time and frequency with the

non-commutative operators $\mathfrak{I}$ and $\mathfrak{R}$, so that

$$\mathfrak{I} \to t, \quad \mathfrak{R} \to -\mathrm{i}\frac{d}{\mathrm{d}t} \text{ in the time domain;}$$

$$\mathfrak{I} \to \mathrm{i}\frac{d}{\mathrm{d}\omega}, \quad \mathfrak{R} \to \omega \text{ in the frequency domain,}$$

where $\mathfrak{I},\mathfrak{R}-\mathfrak{R}\mathfrak{I} = \mathrm{i}$. Introducing the operator $G(\mathfrak{I},\mathfrak{R})$, associated with the function $g(t,\omega)$, one can write

$$\langle g(t,\omega)\rangle = \int_{-\infty}^{\infty} A^*(t)G(t,\mathfrak{R})A(t)\,\mathrm{d}t = \int_{-\infty}^{\infty} S^*(\omega)G(\mathfrak{I},\omega)S(\omega)\,\mathrm{d}\omega. \quad (A.5)$$

Due to the characteristic function is a mathematical expectation, one can apply Eq. (A.5) to estimate $M(\theta,\tau)$ via

$$M(\theta,\tau) = \langle \exp(\mathrm{i}\theta t + \mathrm{i}\tau\omega)\rangle \to \int_{-\infty}^{\infty} A^*(t)\exp(\mathrm{i}\theta\mathfrak{I} + \mathrm{i}\tau\mathfrak{R})A(t)\,\mathrm{d}t. \quad (A.6)$$

In fact, Eq. (A.6) includes the Weil correspondence $\exp(\mathrm{i}\theta t + \mathrm{i}\tau\omega) \to \exp(\mathrm{i}\theta\mathfrak{I} + \mathrm{i}\tau\mathfrak{R})$, but such a correspondence is not a uniquely applicable. In principle, it can be generalized by substituting the normal ordered correspondences that leads to another possible time–frequency distributions [20]. Nevertheless, now we have an opportunity to calculate the characteristic function $M(\theta,\tau)$ using Eq. (A.6). In so doing, one has to take the particular case of well-known Backer–Hausdorff operator formula [21]

$$\exp(\mathrm{i}\theta\mathfrak{I} + \mathrm{i}\tau\mathfrak{R}) = \exp(-\mathrm{i}\theta\tau/2)\exp(\mathrm{i}\tau\mathfrak{R})\exp(\mathrm{i}\theta\mathfrak{I}), \quad (A.7)$$

where $\exp(\mathrm{i}\tau\mathfrak{R})$ is the operator, because

$$\exp(\mathrm{i}\tau\mathfrak{R})A(t) = \exp(\tau d/\mathrm{d}t)A(t) = A(t+\tau). \quad (A.8)$$

Substituting Eq. (A.8) into Eq. (A.6), one can yield

$$M(\theta,\tau) = \int_{-\infty}^{\infty} A^*(t)\exp(-\mathrm{i}\theta\tau/2)\exp(\mathrm{i}\theta t)A(t+\tau)\,\mathrm{d}t. \quad (A.9)$$

At this stage, a new independent variable $u = t-\tau/2$ with $\mathrm{d}u/\mathrm{d}t$ can be introduced, so

$$M(\theta,\tau) = \int_{-\infty}^{\infty} A^*\left(u-\frac{\tau}{2}\right)\exp(\mathrm{i}\theta u)A\left(u+\frac{\tau}{2}\right)\mathrm{d}u. \quad (A.10)$$

Now we use Eq. (A.2) to obtain the time–frequency distribution $W(t,\omega)$

$$W(t,\omega) = \frac{1}{4\pi^2}\int_{-\infty}^{\infty}\int_{-\infty}^{\infty}\int_{-\infty}^{\infty} A^*\left(u-\frac{\tau}{2}\right)\exp(\mathrm{i}\theta u)A\left(u+\frac{\tau}{2}\right) \times \exp(-\mathrm{i}\theta t - \mathrm{i}\tau\omega)\mathrm{d}\theta\,\mathrm{d}\tau\,\mathrm{d}u. \quad (A.11)$$

The integration with respect to θ gives the Dirac delta-function $\delta(u-t)$ in Eq. (A.11), i.e.

$$W(t,\omega) = \frac{1}{2\pi}\int_{-\infty}^{\infty}\int_{-\infty}^{\infty} \delta(u-t)A^*\left(u-\frac{\tau}{2}\right)A\left(u+\frac{\tau}{2}\right) \times \exp(-\mathrm{i}\tau\omega)\mathrm{d}\tau\,\mathrm{d}u. \quad (A.12)$$

Then, integrating with respect to u, we arrive at the Wigner time–frequency distribution

$$W(t,\omega) = \frac{1}{2\pi}\int_{-\infty}^{\infty} A^*\left(t-\frac{\tau}{2}\right)\exp(-\mathrm{i}\tau\omega)A\left(t+\frac{\tau}{2}\right)\mathrm{d}\tau. \quad (A.13)$$

This distribution can be explained in terms of frequency as well by the following integral expression

$$W(t,\omega) = \frac{1}{2\pi}\int_{-\infty}^{\infty} S^*\left(\omega-\frac{\theta}{2}\right)\exp(\mathrm{i}t\theta)S\left(\omega+\frac{\theta}{2}\right)\mathrm{d}\theta. \quad (A.14)$$

The kernel of this distribution is equal to unity, while the kernel of the Wigner transformation depends on the product of the arguments. The power density $|A(t)|^2$ and the spectrum density $|S(\omega)|^2$ are determined by

$$\text{(a)} \quad |A(t)|^2 = \int_{-\infty}^{\infty} W(t,\omega)\,\mathrm{d}\omega,$$

$$\text{(b)} \quad |S(\omega)|^2 = \int_{-\infty}^{\infty} W(t,\omega)\,\mathrm{d}t. \quad (A.15)$$

References

[1] M.B. Priestley, Spectral Analysis and Time Series, Academic Press, London, New York, 1982.

[2] D.B. Percival, A.T. Walden, Spectral Analysis for Physical Applications: Multitaper and Conventional Univariate Techniques, Cambridge University Press, Cambridge, 1993.

[3] P.F. Dunn, Measurement and Data Analysis for Engineering and Science, McGraw-Hill, New York, 2005.

[4] J.-C. Diels, W. Rudolph, Ultrashort Laser Pulse Phenomena: Fundamentals, Techniques and Applications on a Femtosecond Time Scale, Academic Press, Boston, 1996.

[5] K.W. Delong, R. Trebino, Frequency-resolved optical gating with the use of second-harmonic generation, J. Opt. Soc. Am. B 11 (1994) 2206–2215.

[6] C. Iaconis, I.A. Walmsley, Spectral phase interferometry for dielectric electric-field reconstruction of ultrashort optical pulses, Opt. Lett. 23 (1998) 792–794.

[7] J. Dai, H. Teng, Ch. Guo, Second- and third-order interferometric autocorrelations based on harmonic generations from metal surfaces, Opt. Commun. 205 (2005) 173–178.

[8] E.P. Ippen, C.V. Shank, in: S.L. Shapiro (Ed.), Ultrashort Light Pulses, Springer, New York, 1977.

[9] A.S. Shcherbakov, Synchronization of a radio-interferometer by the high-repetition-rate picosecond solitons, Tech. Phys. Lett. 19 (1993) 615–616.
[10] J. Herrmann, B. Wilhelmi, Laser fur Ultrakurze Lichtimpulse, Akademi-Verlag, Berlin, 1984.
[11] D. Dragoman, Redundancy of phase-space distribution functions in complex field recovery problems, Appl. Opt. 42 (11) (2003) 1932–1937.
[12] J.-C. Diels, J.J. Fontaine, I.C. McMichel, Control and measurement of ultrashort pulse shapes (in amplitude and phase) with femtosecond accuracy, Appl. Opt. 24 (1985) 1270–1282.
[13] K. Nagamuna, K. Mogi, H. Yamada, General method for ultrashort light pulse chirp measurement, IEEE J. Quantum Electron. 25 (1989) 1225–1233.
[14] D.J. Kame, R. Trebino, Single-shot measurement of the intensity and phase of a femtosecond laser pulse, Proc. SPIE 1861 (1993) 150–160.
[15] E.L. Portnoy, S.D. Yakubovich, N.M. Stelmakh, Dynamics of emission of radiation from a heterolaser with a saturable absorber formed by deep implantation of oxygen ions, Phys. Semicond. 22 (7) (1998) 766–768.
[16] G.P. Agrawal, N.K. Dutta, Semiconductor Lasers, Van Nostrand Reinhold, New York, 1993.
[17] I.A. Kniazev, A.S. Shcherbakov, Yu.V. Il'in, Picosecond pulse source based on a semiconductor laser with a fiber cavity, Tech. Phys. Lett. 17 (1991) 82–83.
[18] E.I. Andreeva, A.S. Shcherbakov, I.E. Berishev, Semiconductor source of picosecond pulses at a wavelength of 1.55 μm, Tech. Phys. Lett. 18 (1992) 803–804.
[19] A.S. Shcherbakov, E.I. Andreev, Observation of picosecond optical pulses with a guiding-center soliton in a single-mode optical fiber wave-guide, Tech. Phys. Lett. 20 (1994) 873–875.
[20] L. Cohen, Generalized phase-space distribution functions, J. Math. Phys 7 (1996) 781–786.
[21] R.M. Wilcox, Exponential operators and parameter differentiation in quantum physics, J. Math. Phys. 8 (1967) 962–982.